

Electronic Raman scattering in filling-controlled metals: $\text{Sr}_{1-x}\text{La}_x\text{TiO}_3$

T. Katsufuji and Y. Tokura

Department of Physics, University of Tokyo, Tokyo 113, Japan

(Received 13 August 1993; revised manuscript received 28 October 1993)

Electronic Raman scattering has been investigated for metallic $\text{Sr}_{1-x}\text{La}_x\text{TiO}_3$ in which the 3d band filling (x) can be systematically changed from $x = 0$ (a band insulator) to $x = 1$ (a Mott-Hubbard insulator). The symmetry dependence of the scattering intensity can be accounted for in terms of the neutral carrier density fluctuation model. However, a systematic change of the spectral shape with the carrier density ($\simeq x$) is observed. All the spectra can be reproduced by a relaxational function with an ω -dependent scattering rate (Γ). The ω dependence of Γ gets stronger with x , which is in accord with the x -dependent enhancement of the effective mass, due to the electron correlation effect.

Electronic Raman scattering has been experimentally and theoretically studied in various kinds of doped semiconductors.¹ Theoretically, Raman scattering of a free electron gas relates to the density-density correlation function and the spectrum consists of two components: a single-particle excitation with a cutoff at $\omega \sim qv_F$ (where q is a difference between an incident and scattered light momentum and v_F is a Fermi velocity), and a collective excitation of the plasma. In the electronic Raman-scattering process of real doped semiconductors, however, the band structure and/or spin-orbit coupling play an important role and cause a variety of features, depending on the details of the band structure and carrier concentration (n). On the other hand, experimental studies of electronic Raman scattering of metals ($n \sim 10^{22}/\text{cm}^3$) were mainly concentrated on superconductors and their gap spectra, while there have been very few studies on spectra in the normal state. In recent years, the electronic Raman scattering of high- T_c cuprate superconductors has been extensively studied,² especially on their anomalously flat spectra in the normal state.³ Some interpretations based on the strong correlation effect of 3d electrons have been presented to account for the observed unconventional features in the electronic Raman spectra in cuprates.^{4,5}

In order to clarify the electron correlation effect on the electronic Raman scattering of metals, a broader perspective would be needed that may be achieved by systematically varying the band filling or the bandwidth in a specific metal. We propose here the mixed crystal system $\text{Sr}_{1-x}\text{La}_x\text{TiO}_3$ as one of the most suitable systems for such an investigation. Recently, the electronic properties of $\text{Sr}_{1-x}\text{La}_x\text{TiO}_3$ have been extensively studied.^{6,7} In this system, the lattice structure is pseudo simple cubic and the number of 3d electrons per Ti site can be controlled from 0 to 1 by substituting Sr with La. Except near both end compounds, i.e., SrTiO_3 ($x = 0$) which is a band insulator and LaTiO_3 ($x = 1$) which is a Mott insulator with antiferromagnetic ordering below 150 K,⁸ the mixed crystal system shows metallic properties. The most striking feature in the metallic phase is the increase of the carrier effective mass as x (the band filling) increases and approaches 1. This has been assigned to

the correlation of 3d electrons with a narrow bandwidth, which also results in enhancements of Pauli paramagnetic susceptibility and the T^2 coefficient of resistivity.⁶ In this sense, a wide range of metallic state can be realized in the titanate system, from the weakly to highly correlated metal, or from the doped band insulator to doped Mott insulator. Therefore, the system is suitable for the systematic study of electronic Raman scattering in metals by changing the effective strength of the electron correlation. In this paper, we report on the electronic Raman scattering of $\text{Sr}_{1-x}\text{La}_x\text{TiO}_3$ with varying polarization and temperature for various filling levels x .

Samples used in this study were polycrystals that were melt grown by the floating-zone method and details about these samples were described elsewhere.^{6,7} A single crystal of the $x = 0.1$ sample was also prepared by the same method but with a slower feed speed (12 mm/h). The samples with $x=0.1-0.9$ show metallic behavior, and the Hall coefficient (R_H) is negative and the number of carriers per Ti site deduced from $(eR_H)^{-1}$ approximately equals x (within a relative error of 10%), indicating that x is a good measure for the actual carrier density ($n \simeq x$).⁶ All the samples were mechanically polished with alumina powder. The orientation of the single crystal was determined by x-ray back-Laue diffraction measurements and the (110) surface was used for the Raman-scattering measurements. A 514.5 nm line from an argon ion laser was used as an incident light and the nearly backward scattered light was collected and dispersed by a triple monochromator equipped with an intensified-diode-array detector. The absorption coefficients at 514.5 nm (2.41 eV) in these samples are relatively small, especially in the low x region ($\ll 1$), and the optical constants at 2.41 eV derived by Kramers-Kronig analysis of the reflectivity data are not so reliable as to be used for the accurate penetration depth correction of the spectra. Therefore, we did not correct the Raman spectra for the optical response of the crystals at the energy of incident and scattered light, and in consequence we cannot discuss the relative intensity of each sample. However, we can discuss the ω dependence of the spectra for each x , because the optical constants in the energy region of the scattered light (2.3–2.4 eV) can be regarded

as nearly constant in each sample.

In Fig. 1 we show polarized Raman-scattering spectra of the $x = 0.1$ single crystal that has a cubic symmetry at room temperature. We measured the spectra for the following polarization configurations: $[\frac{1}{\sqrt{2}}(x+y) + z, \frac{1}{\sqrt{2}}(x+y) - z] = \frac{3}{4}E_g + \frac{1}{4}T_{2g}$, $[\frac{1}{\sqrt{2}}(x+y), z] = T_{2g}$, and $[\frac{1}{\sqrt{2}}(x+y) + z, \frac{1}{\sqrt{2}}(x+y) + z] = \frac{9}{16}A_{1g} + \frac{1}{12}E_g + \frac{5}{4}T_{2g}$ (where the x, y, z refers to the Ti-O direction). We obtained the pure symmetry components by combining the spectra for these configurations. The $\omega = 0$ centered continuum was observed in the Raman spectra in the E_g and A_{1g} symmetry, whose intensity decreases as $|\omega|$ increases. By contrast, the T_{2g} component bears little intensity. The inset shows the imaginary part of the susceptibility, $\chi''(\omega)$, for the E_g component which relates to the spectral intensity, $\chi''(\omega) = [1 - \exp(-\hbar\omega/kT)] \times I(\omega)$. The symmetrical shape of $\chi''(\omega)$ ensures that this spectrum arises from the scattering of first-order process, and neither from luminescence, Rayleigh scattering, nor scattering of higher-order process.

In this sample ($x = 0.1$), which has a cubic-perovskite structure, there should be no Raman-allowed phonon mode, and the continuum cannot be ascribed to a soft phonon spectrum. In fact, in the Raman spectrum of the band insulator SrTiO_3 ($x = 0$) there is no continuum apart from some two-phonon scattering components.⁹ Therefore, we can attribute the continuum observed in $\text{Sr}_{0.9}\text{La}_{0.1}\text{TiO}_3$ to the single-particle excitations. To explain the symmetry dependence of the continuum, we adopt here the neutral carrier density fluctuation model,¹ which has been applied to the interpretation of the polarization dependence of electronic Raman scattering in heavily doped Si (Ref. 10) and more lately to the case of the high- T_c cuprates.¹¹ According to this model, when the effective mass tensors around the Fermi surface are locally anisotropic, the electronic Raman scattering couples to the neutral charge density fluctuation and the scatter-

ing intensity in the low-frequency region is not suppressed by the Coulomb screening effect.¹² Then, the intensity is given by¹²

$$I \propto \left\langle \left[\vec{e}_S \cdot \left(\frac{1}{\vec{m}} - \left\langle \frac{1}{\vec{m}} \right\rangle \right) \cdot \vec{e}_L \right]^2 \right\rangle, \quad (1)$$

where \vec{e}_L and \vec{e}_S are the polarization vectors of an incident and scattered light, \vec{m} is the effective-mass tensor, and $\langle \dots \rangle$ represents the average over the Fermi surface. With the definition that $\mu_{ij} = \vec{e}_i \cdot \left(\frac{1}{\vec{m}} \right) \cdot \vec{e}_j$, the pure symmetry components are given by the relations

$$A_{1g} = \left\langle \left[\frac{1}{3}(\mu_{11} + \mu_{22} + \mu_{33} - \langle \mu_{11} + \mu_{22} + \mu_{33} \rangle) \right]^2 \right\rangle, \quad (2)$$

$$E_g = \left\langle \left[\frac{1}{2}(\mu_{11} - \mu_{22}) \right]^2 \right\rangle \\ = \left\langle \left[\frac{1}{2\sqrt{3}}(-\mu_{11} - \mu_{22} + 2\mu_{33}) \right]^2 \right\rangle, \quad (3)$$

and

$$T_{2g} = \langle \mu_{12}^2 \rangle = \langle \mu_{23}^2 \rangle = \langle \mu_{31}^2 \rangle. \quad (4)$$

We can easily evaluate the above values based on the tight-binding model on the simple cubic lattice where transfer integrals exist only between nearest-neighbor sites, that is the simplest approximation for the conduction band in the present titanate system. The results are that the T_{2g} component is exactly zero and that the E_g component has a finite value that is larger than that of A_{1g} components. The elaborate band calculation was carried out for SrTiO_3 (Ref. 13) in which the structure of the conduction band resembles the simple tight-binding band as far as the anisotropy of Fermi surface is concerned. Thus, the neutral carrier density fluctuation model predicts that the E_g component is much stronger than the T_{2g} component. This is consistent with our experimental result, indicating that the electronic Raman scattering in this system is dominated by the mechanism of the neutral carrier density fluctuation.

In Fig. 1 we also show the depolarized spectrum (in which the polarization of the incident light is taken to be perpendicular to that of the scattered light) of the polycrystal with the same La concentration ($x = 0.1$). The depolarized configuration should include both the E_g and T_{2g} components but not the A_{1g} ones. The spectrum, if multiplied by an appropriate constant, coincides with E_g spectrum of the single crystal, as can be seen in Fig. 1. Therefore, it is sufficient to measure the depolarized spectra of the polycrystalline samples as far as we discuss the spectral shape of the electronic Raman scattering in $\text{Sr}_{1-x}\text{La}_x\text{TiO}_3$.

Figure 2 shows x -dependent features of the depolarized electronic Raman-scattering spectra, which are perhaps dominated by the E_g component, in the polycrystals at room temperature. (Note that the La concentration x represents the carrier density.) As described above, we cannot discuss the relative intensity of each spectrum. Thus, the scale of the ordinate is in arbitrary units and the scattering intensities for the respective spectra are

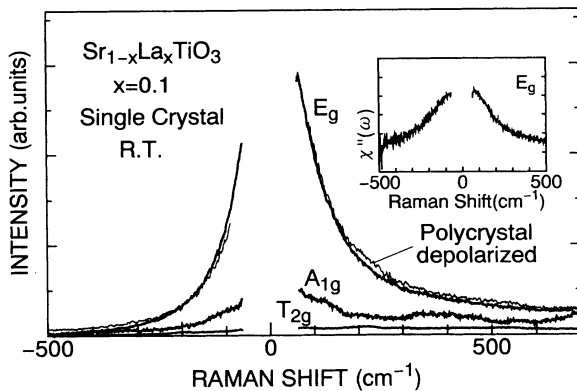


FIG. 1. Raman-scattering spectra of a single crystal $\text{Sr}_{1-x}\text{La}_x\text{TiO}_3$ ($x = 0.1$) at room temperature. The spectra in the negative frequency region correspond to the anti-Stokes component. The E_g , T_{2g} , and A_{1g} symmetry spectra are derived by combining the spectra with several polarization configurations (see text). The inset shows the imaginary part of the susceptibility $\chi''(\omega)$ obtained for the E_g components by the relation $\chi''(\omega) = [1 - \exp(-\hbar\omega/kT)]I(\omega)$.

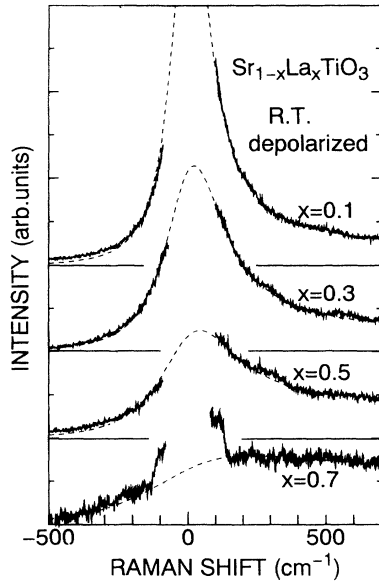


FIG. 2. Raman-scattering spectra of polycrystals $\text{Sr}_{1-x}\text{La}_x\text{TiO}_3$ with various band filling x at room temperature for the depolarized configuration (in which the polarizations of incident and scattered light are perpendicular to each other). Dashed lines represent the results of the fitting, with Eqs. (5) and (6).

normalized at 250 cm^{-1} . In this figure, we clearly see a systematic change of the spectral shape with the band filling x : When x is small, the spectral shape resembles the simple relaxational form which was typically observed in heavily doped n -type Si,¹⁴ and when x is large, the spectral shape is nearly flat which is qualitatively similar to those observed in high- T_c cuprate superconductors.³ We also measured the spectra for $x = 0.7$ in the higher energy region and found that the flat continuum is seen up to 6000 cm^{-1} as in the cuprate superconductors.³

We tried to reproduce these spectra with a simple relaxational form which was previously applied to the case of heavily doped n -type Si.¹⁴ This formula is given with ω independent Γ as

$$I(\omega) = \frac{1}{1 - \exp(-\hbar\omega/kT)} \frac{B\omega\Gamma}{\omega^2 + \Gamma^2}. \quad (5)$$

However, the results of this fitting were unsatisfactory, because the simple relaxational formula can hardly reproduce such nearly flat spectra as observed at large x in $\text{Sr}_{1-x}\text{La}_x\text{TiO}_3$. In turn, we tried to fit all the spectra with the “extended” relaxational formula, which is given as Eq. (5) with ω dependent Γ ;

$$\Gamma = \Gamma_0(T) + \alpha\omega^2, \quad (6)$$

where the simple relaxational form refers to the case of $\alpha = 0$. In the case of high- T_c cuprates, the nearly flat (ω -independent) and temperature (T)-independent spectra can be reproduced by assuming the form of $\Gamma = \sqrt{(\alpha\omega)^2 + (\beta T)^2}$ (Ref. 5), which is in accord with the *marginal Fermi liquid* model.¹⁵ For $\text{Sr}_{1-x}\text{La}_x\text{TiO}_3$, however, a previous study⁶ clearly showed that the Fermi liquid picture holds good in the whole metallic region

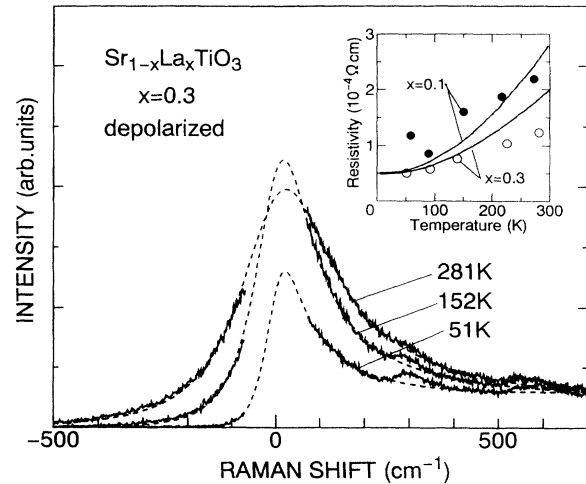


FIG. 3. Raman-scattering spectra of $\text{Sr}_{1-x}\text{La}_x\text{TiO}_3$ ($x = 0.3$) at various temperatures. Dashed lines represent the result of the fitting with Eqs. (5) and (6) in text. The inset shows a comparison between the calculated resistivity by Eq. (7) (open and solid circles) and the measured resistivity (solid lines).

($0.1 \leq x \leq 0.95$) of $\text{Sr}_{1-x}\text{La}_x\text{TiO}_3$. Therefore, we take the ω dependence of Γ as in Eq. (6), which is expected from the Fermi liquid theory.¹⁶ The results of the least square fitting with the three adjustable parameters, $\Gamma_0(T)$, α , and B , are quite satisfactory, and three parameters can be determined with little ambiguity at least for $x \leq 0.5$.¹⁷ The fitted spectra are shown by dashed lines in Fig. 2. In Fig. 3, we also show the temperature dependence of the electronic Raman-scattering spectra of the $x = 0.3$ sample and the results of the same fitting procedure (dashed lines).¹⁸ $\Gamma_0(T)$ in this model should relate to the electrical resistivity,

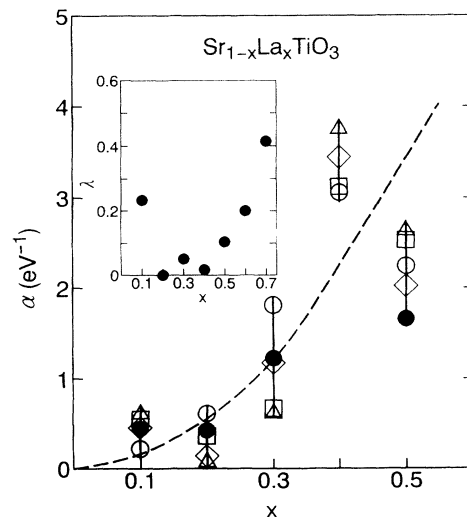


FIG. 4. The ω^2 coefficient (α) of Γ with various band filling x and temperatures obtained by fitting the Raman spectra with Eqs. (5) and (6). The temperatures are the following: ~ 50 (filled circles); ~ 90 (open circles); ~ 150 (open squares); ~ 220 (open rhombuses); ~ 300 K (open triangles). A dashed line is a guide to the eye. The inset shows the enhancement factor (λ) of the effective mass derived by specific-heat measurements in Ref. 6.

$$\rho(T) \simeq \frac{m\Gamma_0(T)}{ne^2} = \frac{4\pi\Gamma_0(T)}{\omega_p^2}. \quad (7)$$

We calculated $\rho(T)$ using the $\Gamma_0(T)$ values obtained by the above fitting procedure and the plasma frequency ω_p ($\hbar\omega_p \simeq 0.58$ eV at $x = 0.1$ and 0.95 eV at $x = 0.3$) estimated by the reflectivity measurements.⁷ Both the calculated and measured values of the resistivity are shown in the inset of Fig. 3. The consistency between the calculated and measured results is satisfactory, which ensures the applicability of this model to the present titanates system.

Figure 4 shows obtained values of the parameter α (i.e., ω^2 coefficient in Γ) at various temperatures and band filling x . Temperature-dependent variation of α within the same x is relatively small, while the x dependence of α is quite remarkable. The relation between α and the spectral shape are summarized as follows: the small α value produces a steep spectrum [as in heavily doped n -type Si (Ref. 14)], whereas the large α value produces a flat spectrum (as in high- T_c superconductors³). In the light of Fermi liquid theory, the α value should be temperature independent and relates to the enhancement of effective mass of carriers.¹⁹ We show in the inset of Fig. 4 the mass enhancement factor λ [which is defined with effective mass (m^*) and noninteracting band mass (m_B) as such that $1 + \lambda = m^*/m_B$] that is derived by the observed values of the electronic specific heat coefficient (γ).²⁰ We clearly see that λ increases as x increases. Therefore, the increase of the α value with x is consistent

with the electron correlation-induced mass enhancement in the present system. The value of λ for $x = 0.1$ is relatively high, indicating the importance of the polaronic effect in the low carrier density region of the quasi ionic crystal. However, the enhancement of the effective mass arising from such an electron-lattice interaction seems not to cause the ω dependence of the Γ over such a large energy scale as observed in the electronic Raman scattering.

In summary, we have investigated the electronic Raman-scattering spectra of $\text{Sr}_{1-x}\text{La}_x\text{TiO}_3$ as a typical system of the filling-controllable metals, with changing polarization symmetry, carrier number, and temperature. The neutral carrier density fluctuation model can explain the symmetry dependence of the scattering intensity. The profile of the electronic Raman spectrum transforms from a relaxational type to a structureless flat shape. All these spectra can be reproduced by the extended relaxational form with the ω -dependent scattering rate; $\Gamma(\omega) = \Gamma_0 + \alpha\omega^2$. The parameter α is an indication of the electron correlation effect and increases as the filling x (or carrier density) increases and as the Mott insulator ($x = 1$) is approached.

We are grateful to Y. Fujishima for his collaboration in sample preparation. We also thank H. Takagi and N. Nagaosa for enlightening discussion. The present work was supported by a Grant-In-Aid for Scientific Research from Ministry of Science, Education and Culture, Japan.

¹ For a review of electronic Raman scattering in doped semiconductors, see M. V. Klein, in *Light Scattering in Solids I*, edited by M. Cardona (Springer, Berlin, 1983), and references therein.

² For a review of electronic Raman scattering in high- T_c superconductors, see C. Thomsen, in *Light Scattering in Solids VI*, edited by M. Cardona and G. Güntherrodt (Springer, Berlin, 1991), and references therein.

³ S. Sugai, Y. Enomoto, and T. Murakami, *Solid State Commun.* **72**, 1193 (1989).

⁴ B. S. Shastry and B. I. Shraiman, *Phys. Rev. Lett.* **65**, 1068 (1990).

⁵ F. Slakey, M. V. Klein, J. P. Rice, and D. M. Ginsberg, *Phys. Rev. B* **43**, 3764 (1991).

⁶ Y. Tokura, Y. Taguchi, Y. Okada, Y. Fujishima, T. Arima, K. Kumagai, and Y. Iye, *Phys. Rev. Lett.* **70**, 2126 (1993).

⁷ Y. Fujishima, Y. Tokura, T. Arima, and S. Uchida, *Phys. Rev. B* **46**, 11167 (1992).

⁸ Y. Okada, T. Arima, Y. Tokura, C. Murayama, and N. Môri, *Phys. Rev. B* **48**, 9677 (1993).

⁹ W. G. Nilsen and J. G. Skinner, *J. Chem. Phys.* **48**, 2240 (1968).

¹⁰ M. Chandrasekhar, M. Cardona, and E. O. Kane, *Phys. Rev. B* **16**, 3579 (1977).

¹¹ T. Katsufuji, Y. Tokura, T. Ido, and S. Uchida, *Phys. Rev. B* **48**, 16131 (1993).

¹² For theoretical studies on this effect in metals, see A. Kawabata, *J. Phys. Soc. Jpn.* **30**, 68 (1971); A. A. Abrikosov and V. M. Genkin, *Zh. Eksp. Teor. Fiz.* **65**, 842 (1973) [*Sov.*

Phys. JETP **38**, 417 (1974)].

¹³ L. F. Mattheiss, *Phys. Rev. B* **6**, 4718 (1972).

¹⁴ G. Contreras, A. K. Sood, and M. Cardona, *Phys. Rev. B* **32**, 924 (1985).

¹⁵ C. M. Varma, P. B. Littlewood, S. Shmidt-Rink, E. Abrahams, and A. E. Ruckenstein, *Phys. Rev. Lett.* **63**, 1996 (1989).

¹⁶ D. Pines and P. Nozières, *The Theory of Quantum Liquids* (Benjamin, New York, 1966).

¹⁷ For the $x = 0.7$ spectra, the ambiguity of the parameters derived by the fitting are quite large. In fact, we can fit the spectrum with another ω -dependent Γ (e.g., ω -linear form) as long as Γ increases sharply as ω increases. Thus, quantitative discussion is difficult in this model when the spectrum is too flat.

¹⁸ The value of B , which is related to the intensity of $\chi''(\omega)$, is almost independent of temperature apart from a small experimental and fitting error. The appearance of the spectra, which decrease in their intensity with lowering temperature, is mainly attributed to the decrease of the Bose factor $[1 - e^{-\hbar\omega/kT}]^{-1}$ with temperature.

¹⁹ K. Miyake, T. Matsuura, and C. M. Varma, *Solid State Commun.* **58**, 507 (1989).

²⁰ The relation between γ and m^* is given as $\gamma \propto (m^*/m_B)n^{1/3} = (1 + \lambda)n^{1/3}$, where n is a carrier density. We calculate the λ value from γ in Ref. 6 by setting $n = x$. We assume that m_B equals the effective mass of the $x = 0.2$ sample, which is the smallest in all x .